NeuroToxicology 59 (2017) 27–32

Contents lists available at ScienceDirect

NeuroToxicology

Brief communication

Compact MRI for the detection of teratoma development following intrathecal human embryonic stem cell injection in NOD-SCID mice

Yuval Ramot[a], Yael S. Schiffenbauer[b], Netanel Amouyal[c], Nathan Ezov[c], Michal Steiner[c], Michal Izrael[d], Neta Lavon[d], Arik Hasson[d], Michel Revel[d], Abraham Nyska[e,*]

[a] Hadassah – Hebrew University Medical Center, Jerusalem, Israel
[b] Aspect Imaging, Shoham, Israel
[c] Envigo CRS (Israel), Ness Ziona, Israel
[d] KadimaStem, Ness Ziona, Israel
[e] Sackler School of Medicine, Tel Aviv University, Tel Aviv, and Consultant in Toxicologic Pathology, Timrat, Israel

ARTICLE INFO

Article history:
Received 2 August 2016
Received in revised form 7 December 2016
Accepted 4 January 2017
Available online 6 January 2017

Keywords:
Stem cells
MRI
Preclinical safety
Teratoma

ABSTRACT

Stem cells are emerging as a promising new treatment modality for a variety of central nervous system disorders. However, their use is hampered by the potential for the development of teratomas and other tumors. Therefore, there is a crucial need for the development of methods for detecting teratomas in preclinical safety studies. The aim of the current study is to assess the ability of a compact Magnetic Resonance Imaging (MRI) system to detect teratoma formation in mice. Five NOD-SCID mice were injected intrathecally with human embryonic stem cells (hESCs), with two mice serving as controls. *In vivo* MRI was performed on days 25 and 48, and *ex vivo* MRI was performed after scheduled euthanization (day 55). MRI results were compared to histopathology findings. Two animals injected with hESCs developed hind-limb paresis and paralysis, necessitating premature euthanization. MRI examination revealed abnormal pale areas in the spinal cord and brain, which correlated histopathologically with teratomas. This preliminary study shows the efficacy of compact MRI systems in the detection of small teratomas following intrathecal injection of hESCs in a highly sensitive manner. Although these results should be validated in larger studies, they provide further evidence that the use of MRI in longitudinal studies offers a new monitoring strategy for preclinical testing of stem cell applications.

1. Introduction

Stem cells are emerging as a new and promising treatment modality for a large number of disorders that involve the central nervous system. These disorders include, for example, traumatic conditions such as spinal cord injury (Barnabe-Heider and Frisen, 2008); degenerative diseases such as amyotrophic lateral sclerosis (Oh et al., 2015), spinocerebellar ataxia (Nakamura et al., 2015) and spinal muscular atrophy (Villanova and Bach, 2015); cerebral hemorrhage (Xue et al., 2014); multiple sclerosis (Izrael et al., 2007) and cerebral palsy (Zali et al., 2015). However, development of such treatments has been hampered by their unfavorable safety risk, and the potential for the development of teratomas or other neoplasms (Cunningham et al., 2012). This risk is especially pronounced when such cells are injected intrathecally, where even the development of small tumors can lead to major health effects, due to the very small free space that is present in the spinal canal (Barnabe-Heider and Frisen, 2008). Unfortunately, such treatments are also being utilized in humans in unauthorized stem-cell clinics (Berkowitz et al., 2016).

It is for this reason that proper preclinical testing is of utmost importance when considering stem cell treatments. Such preclinical assessments include both *in vitro* studies to test for the existence of stem cells, their differentiation and their potential to form tumors, and *in vivo* experiments, using immunocompromised animals (Cunningham et al., 2012; Ramot et al., 2010; Baker and Assaf, 2015). While teratoma formation has been mostly examined in animals in order to assess the pluripotency of stem cells, the formation of such tumors has also been tested as part of preclinical safety assessments (Laflamme et al., 2007; Lu et al., 2009). However, to the best of our knowledge, none of the previous preclinical studies has checked teratoma formation following intrathecal injection (Hentze et al., 2009). Due to the rapid progression in the use of stem cells for central nervous system

* Corresponding author at: Haharuv 18, P.O. Box 184, Timrat, 36576, Israel.
E-mail address: anyska@bezeqint.net (A. Nyska).

http://dx.doi.org/10.1016/j.neuro.2017.01.003
0161-813X/

disorders, it is critical that proper monitoring and assessment tools are utilized in preclinical studies to detect the formation of malignancies and teratomas as early as possible.

Magnetic Resonance Imaging (MRI) is gaining popularity as a potent tool for preclinical toxicologic pathology. It allows the non-invasive monitoring of adverse effects of toxic compounds or drugs, thus eliminating the need for interim euthanizing of animals (Tempel-Brami et al., 2015). It can also help in identifying the location of induced lesions, thereby facilitating the histological assessment of the animals (Tempel-Brami et al., 2015). Furthermore, it can be used to locate injection sites preoperatively (Feng et al., 2014). Two major hurdles limiting the use of MRI in preclinical safety trials have been the relatively high cost of MRI, and its complexity of use. Recently, however, a compact high-performance MRI platform (M-Series system, 1.05 tesla, Aspect Imaging, Shoham, Israel) has been developed to circumvent these hurdles (Taketa et al., 2015; Nyska et al., 2014). Our aim is to assess the ability of the compact MRI to assist in the assessment of teratoma formation following intrathecal injection of pluripotent stem cells in mice.

2. Animals, materials, and methods

2.1. Preparation of human embryonic stem cells (hESCs)

hESCs were expanded in feeder-free, xeno-free growth conditions (Life Technologies). The cells were seeded on vitronectin, grown with E8 media and passaged every 4–5 days using Versene. At seeding, the cells were supplemented with 10uM inhibitor Y27632 (Cayman). Medium was changed daily. Cells were routinely passaged as small clumps with an average split ratio of 1:8. This cell line was tested for its karyotype after 10 passages of growing with the above-detailed conditions and was found to have a normal karyotype. At the day of injection, the hESCs were harvested, counted and resuspended in DMEM/F12 (Life Technologies) to a final concentration of 2×10^8 cells/ml. The cells were kept on ice until transplantation.

2.2. Animals and housing

NOD.CB17-Prkdc^{scid}/NCrHsd male mice, approximately 7–9 weeks old, were obtained from Envigo RMS Ltd (Israel). Animals were acclimatized for laboratory conditions for 6 days. All animals were kept under environmentally-controlled housing conditions throughout the entire study period, set to maintain temperature at 20–24 °C with a relative humidity (RH) of 30–70%, a 12-h light/12-h dark cycle and 15 air changes/h in the study room.

2.3. Experimental design

Two animals were allocated to the vehicle control group, and five animals to the hESC treatment group. Animals were observed up to day 55. 30 min prior to treatment, animals were injected subcutaneously with an opioid analgesic (0.05–0.1 mg/kg of buprenorphine). Afterwards, the animals were anesthetized by isoflurane inhalation (2–3% in oxygen at a flow rate of 0.8-1.2 l/min) and their dorsal skin was clipped of fur using an electric clipper. Thereafter, the clipped area was scrubbed using 4% w/v chlorhexidine gluconate (SEPTAL SCRUB®) and then wiped with ethanol 70%. The animals were placed over a solid platform, enabling curve positioning of the animal's lumbar region. A medial skin incision was performed and retracted to expose the lumbar vertebral column. The inter-vertebral groove between L5 and L6 vertebrae was identified and penetrated using a 30G needle connected to a Hamilton syringe into the spinal canal. The cells or vehicle were injected slowly (over ~30 s). Thereafter, the needle was held for a few more seconds, and a mild pressure was applied once removed. hESC was injected at a dose of 2×10^6 cells/animal (concentration of 2×10^8 cells/ml) to the animals in the treatment group, while control animals were injected with DMEM/F12 alone. All animals were administered at a dose volume of 10 μl/animal. The skin-cut was secured with stainless steel surgical clips and wiped with polydine solution.

Animals were administered Lactated Ringer's Solution (LRS) by subcutaneous injection at a volume dosage of 10 ml/kg immediately after the operation, and allowed to recover over a warm heating pad until full recovery. Chipped pellets of rodent diet were placed on each cage's bottom. Buprenorphine at a dose of 0.05–0.1 mg/kg was injected subcutaneously twice daily for two days.

The study was performed following an application-form review by The National Council for Animal Experimentation and after receiving its approval that the study complies with the rules and regulations set forth in IL-15-03-100.

2.4. Viability, clinical signs and weight

Detailed clinical examinations of the animals were carried out once daily, 5 days a week. Cage-side observations were carried out on the other two days. Observations included changes in skin, fur, eyes, mucous membranes, occurrence of secretions and excretions (e.g. diarrhea) and autonomic activity (e.g. lacrimation, salivation, piloerection, unusual respiratory pattern). Changes in gait, posture and response to handling, as well as the presence of bizarre behavior, tremors, convulsions, sleep and coma were also inspected. All animals were weighed prior to dosing procedure, twice weekly thereafter, and prior to their scheduled euthanization, or prior to removal from the study due to animal welfare reasons.

2.5. In vivo *MRI*

In vivo MRI was performed 25 and 48 days after cell injection, using the M2^{TM} compact MRI system (Aspect Imaging, Israel), equipped with a 35 mm mouse whole body coil, and a 20 mm mouse head coil. Animals were kept anesthetized with 2% isoflorane in O_2 and placed on a specially-designed heated bed where physiological signals were monitored throughout the experiment to ensure the animals' well-being. All experiments were performed in accordance with the guidelines and approval of the Animal Care and Use Committees of the various organizations providing the animal models. Please refer to the specific MR sequence parameters in the correspondent figure legend.

2.6. Ex vivo *MRI*

High-resolution *ex vivo* MRI of formalin fixed brains and spinal cords was performed after sacrifice on day 55, on the same M2^{TM} compact system equipped with a 20 mm RF coil (Tempel-Brami et al., 2015). Samples were fixed using conventional immersion fixation techniques, transferred to phosphate buffered saline or saline for 24 h and then into an MR transparent solution (Fluorinert FC, 3 M, USA) to avoid tissue dehydration. The specific MR sequence parameters are included in the correspondent figure legend.

2.7. Image processing and quantification

Segmentation and volumetric quantification of the digital 3D MRI data was performed using VivoQuant (InviCRO, Boston, USA), an extensive image processing and analysis software package that is fully integrated into the M2^{TM} imaging system.

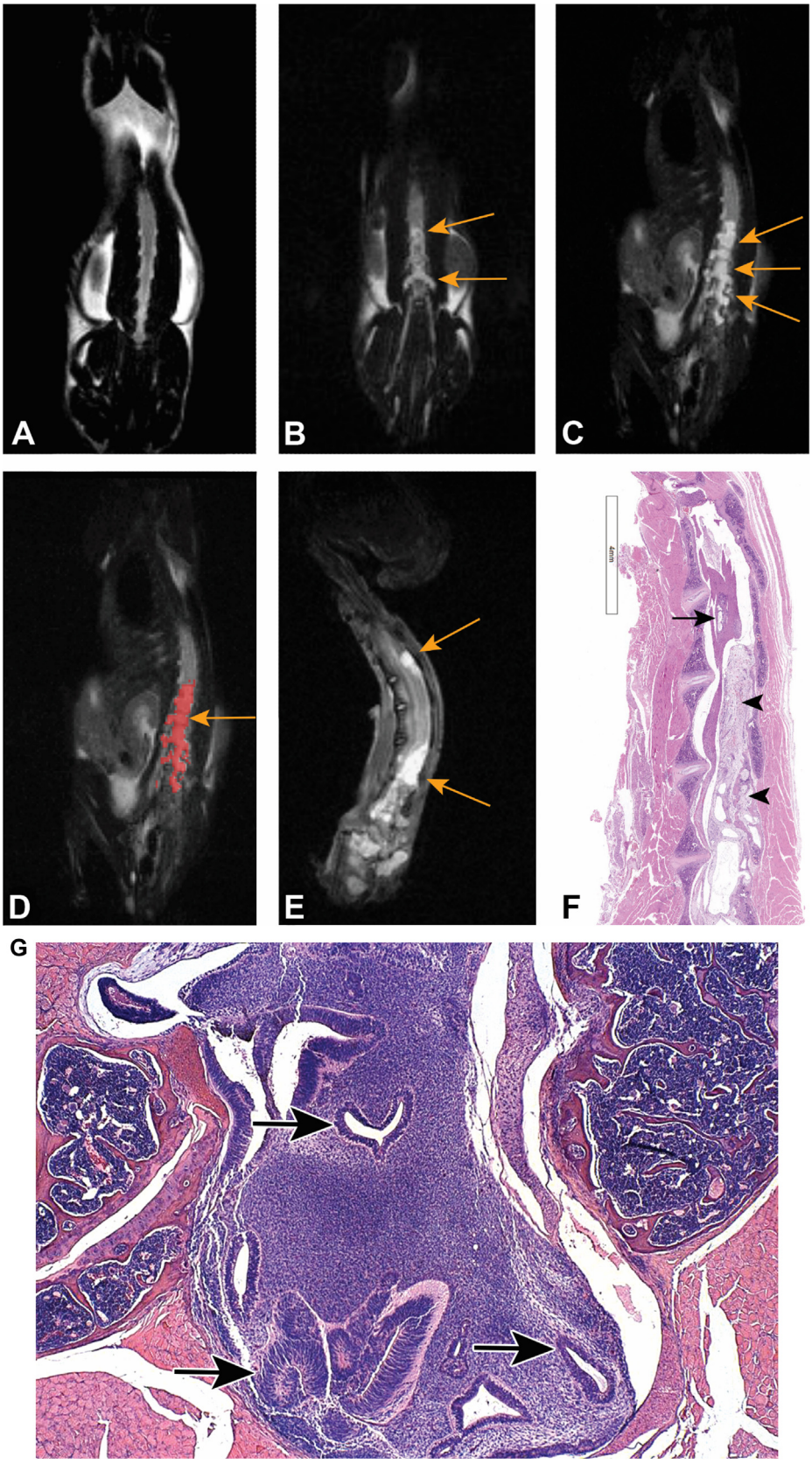

Fig. 1. *In vivo* coronal view (A) of a control animal. *In vivo* coronal view (B–D) and *ex vivo* sagittal view (E) MRI of the spinal cord of a NOD-SCID mouse 25 (B) and 48 (C–E) days after intrathecal injection of hESCs. Note the bright lesion (arrows) located in the lumbar regions, which expanded from day 25–48. Intensity-based segmentation (D) allowed for quantitative assessment of the lesion (i.e. ROI) found to have a volume of 82.62 μl and confirmed by histology to consist of malignant teratoma (F; arrow – teratoma invading the spinal cord; arrowheads – teratoma invading the vertebra and compressing the spinal cord). MRI acquisition parameters: *In vivo* (B–D): Fast Spin Echo, TE 80 ms; TR 2400 ms; Slice thickness 1 mm; Field of view 70 mm; Matrix size 200 × 192; acquisition time 5.5 min *Ex vivo* (E): Fast Spin Echo, TE 74 ms; TR 3000 ms; Slice thickness

2.8. Necropsy and tissue handling

All animals (including animals that were removed from the study for animal welfare reasons) were subjected to a full detailed necropsy and gross pathological examination following the respective scheduled termination (day 55). At necropsy, animals were subjected to thorough examination, including the external surface of the body, all orifices, cranial, thoracic and abdominal cavities and their contents, with particular attention to any evident external macroscopic changes of the injection site and particularly in respect to any evidence of abnormal tissue or tumor formation. All abnormalities and gross pathological changes observed in tissues and/or organs were recorded accordingly.

The injection site and brain were collected from all animals and fixed in 10% neutral buffered formalin (approximately 4% formaldehyde solution). In order to avoid damaging the brain, the calvarium was firstly peeled off, and the entire head was fixed in formalin for at least an overnight period. Thereafter, the brain was gently separated from the skull, and retained with the olfactory bulbs. Following *ex vivo* MRI of brains and spinal cords, histopathological examinations of the brain and the injection site were performed. Tissues were trimmed (7 sections from each brain, 3 transverse sections from each injection site after decalcification), embedded in paraffin, sectioned at approximately 5 μm thickness and stained with Hematoxylin & Eosin (H&E).

3. Results

3.1. Survival, clinical observations, and body and organ weight

Two animals from the treatment group were euthanized for humane reasons prior to study termination on study days 48 and 53. Both animals exhibited hind-limb paresis (uni/bilateral), paralysis, limp tail, inability to abduct the hind limbs' digits and marked decrease in body weight. All other animals survived until study termination, and did not show any abnormal clinical signs or a decrease in body weight.

3.2. Macroscopic observations

A round mass was observed between the right and left brain hemispheres of the male mouse that was euthanized on day 53, proximal to the cerebellum. The mass had a cyst-like structure and measured ~3 mm in diameter. In addition, repletion of the animal's urinary bladder was noted in this animal. No gross lesions were observed in all other animals from either the treatment or vehicle control groups.

3.3. MR imaging

In vivo and *ex vivo* MRI revealed bright irregular areas in the lumbar vertebral region which expanded over time (Fig. 1B–E) in 2 animals of the treated group, the same two animals that exhibited abnormal clinical signs. In one animal, similar lesions were also observed in various regions in the brain (Fig. 2A–C),

3.4. Microscopic observations

Histopathological examination of the two treated animals that were euthanized prematurely confirmed that the pale areas detected by the MRI in the spinal cord and vertebra (Fig. 1F) and brain (Fig. 2D) were malignant teratoma (Dixon et al., 2014; Mohr, 2001). The teratomas showed relatively minor degree of differentiation. It was possible to distinguish tissue derived from the three germ layers, in particular, structures suggesting primitive neuroectodermal tissue, consisting of neural-tube and rosette–like structures (Fig. 1G); mesodermal tissue components, characterized by cellular fibrous stroma–like areas; and endodermal–like components, characterized by the presence of cystic structures lined by flattened to cuboidal, epithelial–like cells. The tumor demonstrated local invasiveness, involving the lumbar spinal cord and surrounding vertebral tissue (i.e., marrow cavity and bone). No lesions were noted in the brain and spinal cord in a single control animal.

4. Discussion

The increasing use of stem cell therapy for different medical indications, and especially for neurological diseases, necessitates the performance of adequate preclinical safety studies. The main concern with the use of stem cells in humans is the formation of teratomas, benign neoplastic tumors, which contain tissue from all three germ layers (Ben-David and Benvenisty, 2011). Several methods have been suggested to assess for teratoma formation in preclinical safety studies, such as the detection of tumor proteins using ELISA (St Ledger et al., 2009). However, the usefulness of serum biomarkers for the detection of teratomas is limited, since small or immature teratomas may have low secretion levels (Ahrlund-Richter and Hendrix, 2014). Indeed, in a recent study, MRI was able to detect such an immature teratoma following injection of induced pluripotent stem cells into immunocompromised rat hearts, which was not evident using a series of selected biomarkers (Riegler et al., 2016).

While MRI has been in wide use for tracking stem cells after their transplantation (Hong et al., 2010), the use of MRI for teratoma detection as part of preclinical safety studies has been reported only sporadically in the literature. Routine MRI examinations were used successfully to detect teratomas following undifferentiated mouse ESCs injection into the striatum of a mouse model of Parkinson's disease (Acquarone et al., 2015) and induced pluripotent stem cell injection to rats with Parkinson's-like pathology (Chang et al., 2012). It is possible that this imaging modality has not been used more frequently due to the high cost and complexity of using previously-available MRI systems. The development of easy-to-use, compact MRI systems can provide researchers and the pharmacology industry with significantly improved tools to assess the potential toxicity of injected stem cells and additional treatments (Tempel-Brami et al., 2015). To the best of our knowledge, our study is the first to report the use of MRI for the detection of teratoma following intrathecal injection of ESCs (Hentze et al., 2009).

Very little is known on the clinical presentation of brain and spine tumors in the context of stem cell transplantation in humans, as this treatment method has been reported only sparsely in the medical literature (Bowman et al., 2015). Nevertheless, recently, Berkowitz et al. (2016) reported on a patient that was treated with intrathecal injections of stem cells, and developed glioproliferative lesions in the spinal cord. This patient demonstrated clinical findings similar to the ones observed in the mice in our model, including development of paresis and urinary bladder malfunction. This report emphasizes the utility of this mouse model for the risks inherent with the use of intrathecal stem cell injections in humans.

Johnson et al. (2014) recently tested the feasibility of application of magnetic resonance histology (MRH), utilizing the 7T horizontal bore magnet, for quantitative assessment of the effects of CNS toxicants (8 mg/kg and 12 mg/kg trimethyltin) in rat

0.7 mm; Field of view 45 mm; Matrix size 256 × 250; acquisition time 63 min. (G) Higher magnification photo (×40) of the teratoma invading into the spinal cord. Note (arrows) structures suggesting primitive neuroectodermal tissue, consisting of neural-tube and rosette–like structures.

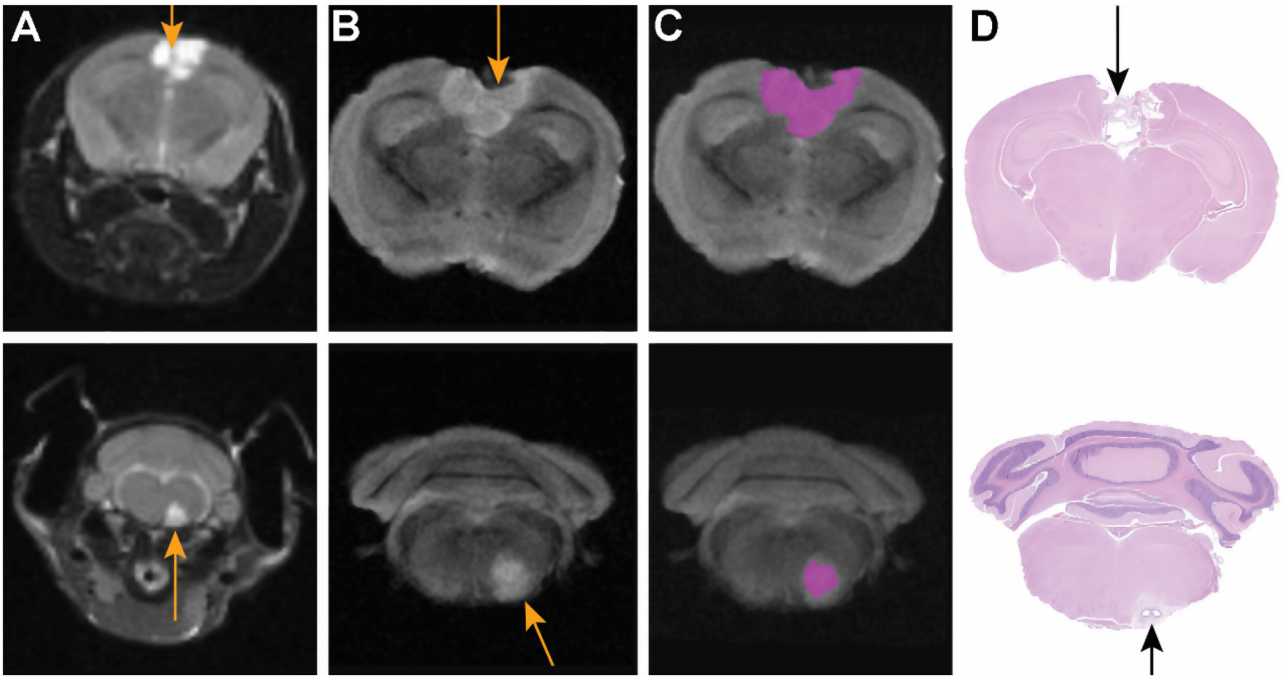

Fig. 2. *In vivo* MRI day 48 (A), *ex vivo* MRI day 55 (B–C) and Histopathology (D) of 2 different areas of the brain of a NOD-SCID mouse 48 days after intrathecal injection of hESCs, showing distinctive lesions. Intensity-based segmentation (C) was performed in order to get quantitative information of the lesions, found to have a total volume (i.e. ROI) of 9.79 μl and confirmed by histology to consist of malignant teratoma (D; Note the presence of cystic structures, arrows). MRI acquisition parameters: *In vivo* (A): Fast Spin Echo, TE 74 ms; TR 2400 ms; Slice thickness 1 mm; Field of view 45 mm; Matrix size 256 × 250; acquisition time 8.5 min. *Ex vivo* (B, C): Fast Spin echo, TE 72 ms; TR 2000 ms; Slice thickness 0.6 mm; Field of view 20 mm; Matrix size 200 × 200; acquisition time 61 min.

models. They showed that subtle and sparse changes to brain structure can be detected using MRH, and correspond to some of the locations in which lesions are found by traditional pathological examination. The authors concluded that MRH brings a valuable addition to pathology with the ability to generate brain-wide quantitative parametric maps for markers of toxic insults in the rodent brain.

In contrast to the MRI scanning utilized by Johnson et al. (2014), we performed the scanning on a 1T magnet system, and the current study demonstrates the effectiveness of compact MRI systems for the detection of small teratomas following intrathecal injection of hESCs in a highly sensitive manner with acquisition times of 5.5 min *in vivo* and 61–63 min *ex vivo*. Compact MRI systems have the advantage of being able to operate in most conventional labs without the cost, complexity, and infrastructure needs of conventional MRI systems.

Here we provide preliminary evidence that intrathecal injection of ESC, when combined with screening by MRI, is a sensitive and quick assay for the detection of teratoma *in vivo*. While the length of most *in vivo* teratoma formation assays is approximately two-to-three months (Gropp et al., 2012; Tang et al., 2012; Zhang et al., 2008), here, teratomas could already be observed after 25 days following injections. Therefore, this mode of administration could be considered for future assays evaluating the safety of ESCs not intended solely for treatment of CNS diseases, but for other indications as well.

The use of repeated MRI imaging offers a new monitoring strategy for preclinical testing of stem cell applications, which is of special importance when these cells are injected into the narrow spinal cord, where even small tumors can result in significant health implications. However, it is important to emphasize that while MRI is highly useful for the accurate localization of potential tumors, it is still necessary to validate each of the altered sites by histopathological examination, in order to clarify the nature of the lesions. This conclusion is consistent with the recent Hanig et al. (Hanig et al., 2014) investigation, stating that "...The traditional neurotoxicologic approach of selecting a few arbitrary brain sections is dramatically improved by MRI targeting that can indicate the location(s) at which to collect 'smart sections' for subsequent workup".

As has been demonstrated in the current report, although MRI can provide highly useful information, and can greatly facilitate preclinical toxicology studies, its use is currently not good laboratory practice (GLP)-compliant. Therefore, when submitted to regulatory agencies, data obtained from MRI analyses are included as non-GLP components within a GLP study. Since imaging in general, and MRI specifically, is highly translatable to clinical settings, its incorporation in such preclinical studies can be of great benefit to regulatory submissions.

This report focused on the use of compact MRI for the detection of teratomas; however, MRI can be a very important adjunct for other carcinogenicity studies. Compact MRI has already been shown to be of benefit for quantifying the volume of preneoplastic changes in liver and kidney carcinogenesis models (Tempel-Brami et al., 2015). MRI can be used for following the growth of local tumors, thus enabling determination between benign tumors and fast-growing malignant lesions (Liu et al., 2015). The fact that MRI can cover the whole body of the animal enables the evaluation of the effects of tumors on adjacent tissues and the overall systemic condition of the animal. The addition of specific contrast agents can also give functional information regarding the tumors in the animal (Ni et al., 2009). Such methods, in addition to dynamic contrast enhanced-MRI for example, can be used for real-time follow-up of the therapeutic effects of different anti-cancer treatments (Wang et al., 2011). Based on the accumulating information on the utility of MRI and compact MRI systems for the detection and volume measurement of preneoplastic and neoplastic changes, it is evident that *in vivo* and *ex vivo* MRI can be applied to carcinogenicity studies.

This preliminary study shows the efficacy of compact MRI systems in the detection of small teratomas following intrathecal injection of hESCs in a highly sensitive manner. Additional studies, incorporating larger numbers of animals and imaging sessions, are needed to better elucidate the earliest time point at which teratomas can be detected by MRI and to validate these results. However, this report can serve as a proof of concept that the use of MRI in longitudinal studies offers a new monitoring strategy for preclinical testing of stem cell applications.

Funding disclosure

The study was funded in part by Aspect Imaging.

References

Acquarone, M., de Melo, T.M., Meireles, F., Brito-Moreira, J., Oliveira, G., Ferreira, S.T., Castro, N.G., Tovar-Moll, F., Houzel, J.C., Rehen, S.K., 2015. Mitomycin-treated undifferentiated embryonic stem cells as a safe and effective therapeutic strategy in a mouse model of Parkinson's disease. Front. Cell. Neurosci. 9, 97.
Ahrlund-Richter, L., Hendrix, M.J., 2014. Oncofetal signaling as a target for cancer therapy. Semin. Cancer Biol. 29, 1–2.
Baker, J.F., Assaf, B.T., 2015. Preclinical study design for evaluation of stem cell-derived cellular therapy products: a pathologist's perspective. Toxicol. Pathol. 43, 126–131.
Barnabe-Heider, F., Frisen, J., 2008. Stem cells for spinal cord repair. Cell Stem Cell 3, 16–24.
Ben-David, U., Benvenisty, N., 2011. The tumorigenicity of human embryonic and induced pluripotent stem cells. Nat. Rev. Cancer 11, 268–277.
Berkowitz, A.L., Miller, M.B., Mir, S.A., Cagney, D., Chavakula, V., Guleria, I., Aizer, A., Ligon, K.L., Chi, J.H., 2016. Glioproliferative lesion of the spinal cord as a complication of stem-Cell tourism. N. Engl. J. Med..
Bowman, M., Racke, M., Kissel, J., Imitola, J., 2015. Responsibilities of health care professionals in counseling and educating patients with incurable neurological diseases regarding stem cell tourism: caveat emptor. JAMA Neurol. 72, 1342–1345.
Chang, Y.L., Chen, S.J., Kao, C.L., Hung, S.C., Ding, D.C., Yu, C.C., Chen, Y.J., Ku, H.H., Lin, C.P., Lee, K.H., Chen, Y.C., Wang, J.J., Hsu, C.C., Chen, L.K., Li, H.Y., Chiou, S.H., 2012. Docosahexaenoic acid promotes dopaminergic differentiation in induced pluripotent stem cells and inhibits teratoma formation in rats with Parkinson-like pathology. Cell Transplant. 21, 313–332.
Cunningham, J.J., Ulbright, T.M., Pera, M.F., Looijenga, L.H., 2012. Lessons from human teratomas to guide development of safe stem cell therapies. Nat. Biotechnol. 30, 849–857.
Dixon, D., Alison, R., Bach, U., Colman, K., Foley, G.L., Harleman, J.H., Haworth, R., Herbert, R., Heuser, A., Long, G., Mirsky, M., Regan, K., Van Esch, E., Westwood, F. R., Vidal, J., Yoshida, M., 2014. Nonproliferative and proliferative lesions of the rat and mouse female reproductive system. J. Toxicol. Pathol. 27, 1S–107S.
Feng, M., Li, Y., Han, Q., Bao, X., Yang, M., Zhu, H., Li, Q., Wei, J., Ma, W., Gao, H., An, Y., Zhao, R.C., Qin, C., Wang, R., 2014. Preclinical safety evaluation of human mesenchymal stem cell transplantation in cerebrum of nonhuman primates. Int. J. Toxicol. 33, 403–411.
Gropp, M., Shilo, V., Vainer, G., Gov, M., Gil, Y., Khaner, H., Matzrafi, L., Idelson, M., Kopolovic, J., Zak, N.B., Reubinoff, B.E., 2012. Standardization of the teratoma assay for analysis of pluripotency of human ES cells and biosafety of their differentiated progeny. PLoS One 7, e45532.
Hanig, J., Paule, M.G., Ramu, J., Schmued, L., Konak, T., Chigurupati, S., Slikker Jr., W., Sarkar, S., Liachenko, S., 2014. The use of MRI to assist the section selections for classical pathology assessment of neurotoxicity. Regul. Toxicol. Pharmacol. 70, 641–647.
Hentze, H., Soong, P.L., Wang, S.T., Phillips, B.W., Putti, T.C., Dunn, N.R., 2009. Teratoma formation by human embryonic stem cells: evaluation of essential parameters for future safety studies. Stem Cell Res. 2, 198–210.
Hong, H., Yang, Y., Zhang, Y., Cai, W., 2010. Non-invasive imaging of human embryonic stem cells. Curr. Pharm. Biotechnol. 11, 685–692.
Izrael, M., Zhang, P., Kaufman, R., Shinder, V., Ella, R., Amit, M., Itskovitz-Eldor, J., Chebath, J., Revel, M., 2007. Human oligodendrocytes derived from embryonic stem cells: effect of noggin on phenotypic differentiation in vitro and on myelination in vivo. Mol. Cell Neurosci. 34, 310–323.
Johnson, G.A., Calabrese, E., Little, P.B., Hedlund, L., Qi, Y., Badea, A., 2014. Quantitative mapping of trimethyltin injury in the rat brain using magnetic resonance histology. Neurotoxicology 42, 12–23.
Laflamme, M.A., Chen, K.Y., Naumova, A.V., Muskheli, V., Fugate, J.A., Dupras, S.K., Reinecke, H., Xu, C., Hassanipour, M., Police, S., O'Sullivan, C., Collins, L., Chen, Y., Minami, E., Gill, E.A., Ueno, S., Yuan, C., Gold, J., Murry, C.E., 2007. Cardiomyocytes derived from human embryonic stem cells in pro-survival factors enhance function of infarcted rat hearts. Nat. Biotechnol. 25, 1015–1024.
Liu, Y., Yin, T., Feng, Y., Cona, M.M., Huang, G., Liu, J., Song, S., Jiang, Y., Xia, Q., Swinnen, J.V., Bormans, G., Himmelreich, U., Oyen, R., Ni, Y., 2015. Mammalian models of chemically induced primary malignancies exploitable for imaging-based preclinical theragnostic research. Quant. Imaging Med. Surg. 5, 708–729.
Lu, B., Malcuit, C., Wang, S., Girman, S., Francis, P., Lemieux, L., Lanza, R., Lund, R., 2009. Long-term safety and function of RPE from human embryonic stem cells in preclinical models of macular degeneration. Stem Cells 27, 2126–2135.
Mohr, U. (Ed.), 2001. International Classification of Rodent Tumors. The Mouse, Springer-Velag, Berlin, Germany.
Nakamura, K., Mieda, T., Suto, N., Matsuura, S., Hirai, H., 2015. Mesenchymal stem cells as a potential therapeutic tool for spinocerebellar ataxia. Cerebellum 14, 165–170.
Ni, Y., Wang, H., Chen, F., Li, J., DeKeyzer, F., Feng, Y., Yu, J., Bosmans, H., Marchal, G., 2009. Tumor models and specific contrast agents for small animal imaging in oncology. Methods 48, 125–138.
Nyska, A., Schiffenbauer, Y.S., Brami, C.T., Maronpot, R.R., Ramot, Y., 2014. Histopathology of biodegradable polymers: challenges in interpretation and the use of a novel compact MRI for biocompatibility evaluation. Polymer. Adv. Tech. 25, 461–467.
Oh, K.W., Moon, C., Kim, H.Y., Oh, S.I., Park, J., Lee, J.H., Chang, I.Y., Kim, K.S., Kim, S.H., 2015. Phase I trial of repeated intrathecal autologous bone marrow-derived mesenchymal stromal cells in amyotrophic lateral sclerosis. Stem Cells Transl. Med. 4, 590–597.
Ramot, Y., Steiner, M., Morad, V., Leibovitch, S., Amouyal, N., Cesta, M.F., Nyska, A., 2010. Pulmonary thrombosis in the mouse following intravenous administration of quantum dot-labeled mesenchymal cells. Nanotoxicology 4, 98–105.
Riegler, J., Ebert, A., Qin, X., Shen, Q., Wang, M., Ameen, M., Kodo, K., Ong, S.G., Lee, W. H., Lee, G., Neofytou, E., Gold, J.D., Connolly, A.J., Wu, J.C., 2016. Comparison of magnetic resonance imaging and serum biomarkers for detection of human pluripotent stem cell-Derived teratomas. Stem Cell Rep. 6, 176–187.
St Ledger, K., Agee, S.J., Kasaian, M.T., Forlow, S.B., Durn, B.L., Minyard, J., Lu, Q.A., Todd, J., Vesterqvist, O., Burczynski, M.E., 2009. Analytical validation of a highly sensitive microparticle-based immunoassay for the quantitation of IL-13 in human serum using the Erenna immunoassay system. J. Immunol. Methods 350, 161–170.
Taketa, Y., Shiotani, M., Tsuru, Y., Kotani, S., Osada, Y., Fukushima, T., Inomata, A., Hosokawa, S., 2015. Application of a compact magnetic resonance imaging system for toxicologic pathology: evaluation of lithium-pilocarpine-induced rat brain lesions. J. Toxicol. Pathol. 28, 217–224.
Tang, C., Weissman, I.L., Drukker, M., 2012. The safety of embryonic stem cell therapy relies on teratoma removal. Oncotarget 3, 7–8.
Tempel-Brami, C., Schiffenbauer, Y.S., Nyska, A., Ezov, N., Spector, I., Abramovitch, R., Maronpot, R.R., 2015. Practical applications of in vivo and ex vivo MRI in toxicologic pathology using a novel high-performance compact MRI system. Toxicol. Pathol. 43, 633–650.
Villanova, M., Bach, J.R., 2015. Allogeneic mesenchymal stem cell therapy outcomes for three patients with spinal muscular atrophy type 1. Am. J. Phys. Med. Rehabil. 94, 410–415.
Wang, H., Marchal, G., Ni, Y., 2011. Multiparametric MRI biomarkers for measuring vascular disrupting effect on cancer. World J. Radiol. 3, 1–16.
Xue, Y.Z., Li, X.X., Li, L., Pang, S.L., Yao, J.G., Hao, P.L., 2014. Curative effect and safety of intrathecal transplantation of neural stem cells for the treatment of cerebral hemorrhage. Genet. Mol. Res. 13, 8294–8300.
Zali, A., Arab, L., Ashrafi, F., Mardpour, S., Niknejhadi, M., Hedayati-Asl, A.A., Halimi-Asl, A., Ommi, D., Hosseini, S.E., Baharvand, H., Aghdami, N., 2015. Intrathecal injection of CD133-positive enriched bone marrow progenitor cells in children with cerebral palsy: feasibility and safety. Cytotherapy 17, 232–241.
Zhang, W.Y., de Almeida, P.E., Wu, J.C., 2008. Teratoma Formation: A Tool for Monitoring Pluripotency in Stem Cell Research. StemBook, Cambridge, MA.